ADVANCED FUNCTIONAL MATERIALS

Supporting Information

for *Adv. Funct. Mater.*, DOI 10.1002/adfm.202302936

Magnetic Nanoislands in a Morphotropic Cobaltite Matrix

Shengru Chen, Dongke Rong, Yan-Xing Shang, Miming Cai, Xinyan Li, Qinghua Zhang, Shuai Xu, Yue Xu, Hanbin Gao, Haitao Hong, Ting Cui, Qiao Jin, Jia-Ou Wang, Lin Gu, Qiang Zheng, Can Wang, Jinxing Zhang, Gang-Qin Liu, Kui-Juan Jin and Er-Jia Guo**

Supporting Information

Magnetic Nanoislands in a Morphotropic Cobaltite Matrix

Shengru Chen,† Dongke Rong,† Yan-Xing Shang, Miming Cai, Xinyan Li, Qinghua Zhang, Shuai Xu, Yue Xu, Hanbin Gao, Haitao Hong, Ting Cui, Qiao Jin, Jia-Ou Wang, Lin Gu, Qiang Zheng, Can Wang, Jinxing Zhang, Gang-Qin Liu, Kui-juan Jin, and Er-Jia Guo**

†These authors contribute equally to the manuscript.

* Correspondence and requests for materials should be addressed to K. J. Jin and E. J. Guo

E-mail: kjjin@iphy.ac.cn and ejguo@iphy.ac.cn

This PDF file includes:

Supplementary Figures S1 to S10.

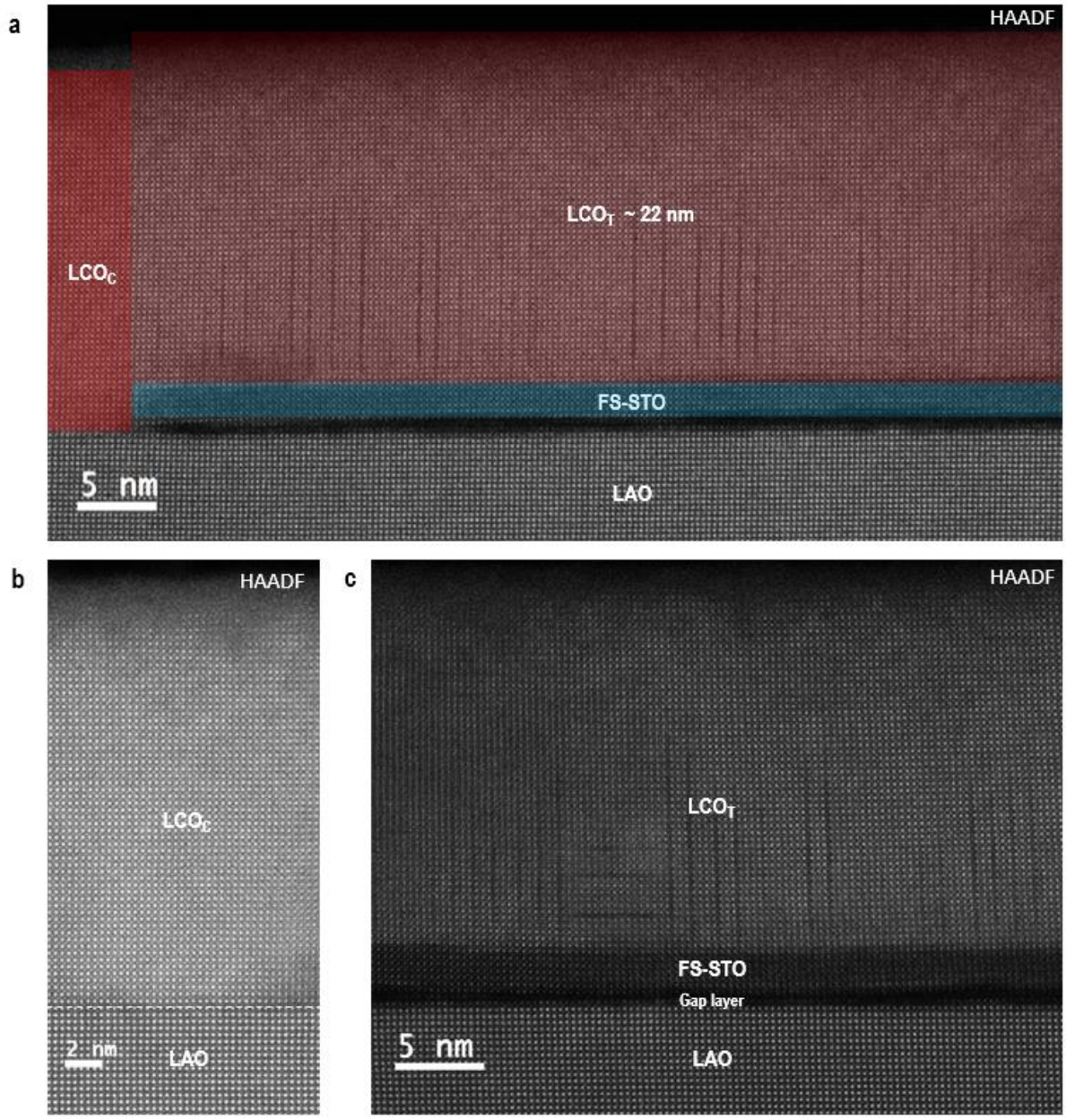

Figure S1. Microscopic structural characterization of a LCO hybrid structure. High-magnified cross-sectional HAADF-STEM images of (a) a LCO hybrid structure at a representative grain boundary region, (b) a LCO_C layer grown directly on LAO substrates, and (c) a LCO_T layer epitaxially grown on FS-STO membranes transferred on LAO substrates. The thickness of LCO_C and LCO_T layers is approximately 22 nm. The FS-STO membranes with a thickness of ~ 6 unit cells are continuous and flat. It covers partial surface of LAO substrates, leaving a space gap layer with thickness less than 1 nm. Apparently, the LCO_C layers are absent from dark strips, where the LCO_T layers contain vertical aligned dark strips. This behavior demonstrates that the LCO layers exhibit distinct strain states laterally depending on their substrates/membranes underneath. Please note that the dark strips in LCO_T layers only persist approximately one half of entire layers. This case is different from previous work that the dark stripes occupy the entire LCO single films grown on STO substrates. We attribute this behavior to the partial relaxation of epitaxial strain provided by FS-STO membranes.

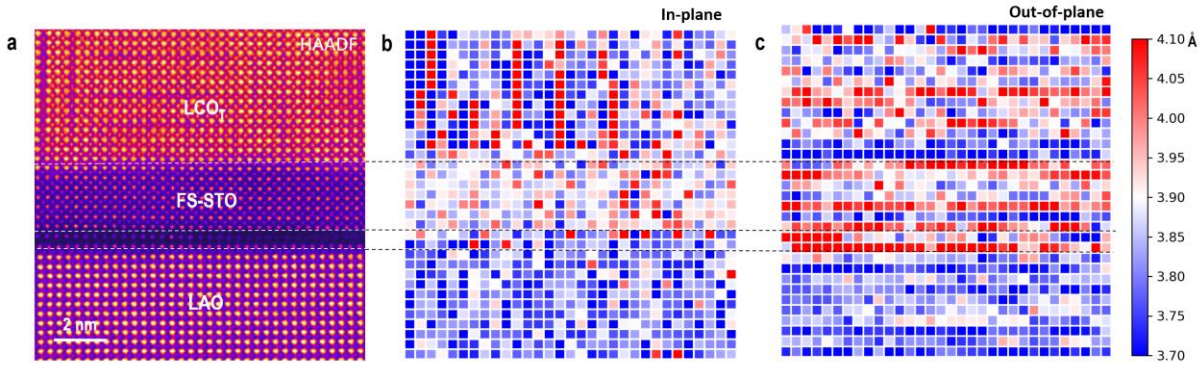

Figure S2. Strain analysis of LCO$_T$ layer grown on FS-STO membranes. (a) High-magnified HAADF-STEM image at LCO$_T$/FS-STO/LAO interface region. The black area is the interfacial gap layer between FS-STO membranes and LAO substrates. (b) and (c) Atomic distance between nearby A-cite elements along the in-plane and out-of-plane direction, respectively. We found that the out-of-plane lattice constant of FS-STO is larger than its in-plane lattice constant. Obviously, this result can only be attributed to the as-grown LCO$_T$ layers reversely apply a compressive-strain to the ultrathin FS-STO membranes. Meanwhile, the in-plane lattice constant of LCO$_T$ layers is slightly smaller than the out-of-plane ones.

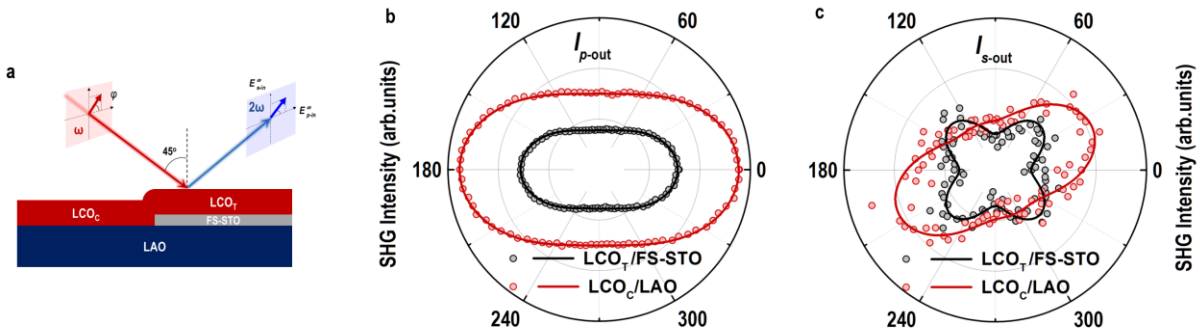

Figure S3. SHG polarimetry of a LCO hybrid structure. (a) Schematic of SHG measurements performed in reflection mode. The incident angle of 800 nm fs-laser is set to 45^{o} with respect to the sample's surface normal. The measurements were repeated in both LCO_C and LCO_T regions at room temperature. (b) and (c) $I_{p\text{-}out}$ and $I_{s\text{-}out}$ components of SHG signal were plotted as function of polarization angle (φ), respectively. Red and black open symbols represent the experimental data obtained from LCO_C and LCO_T regions, respectively. Solid lines are the best fit to the SHG data and plotted for guide. We find that the SHG signal of LCO_T layers can fit the point group symmetry *P*4*mm*, where that of LCO_C fit the point group symmetry *m* better.

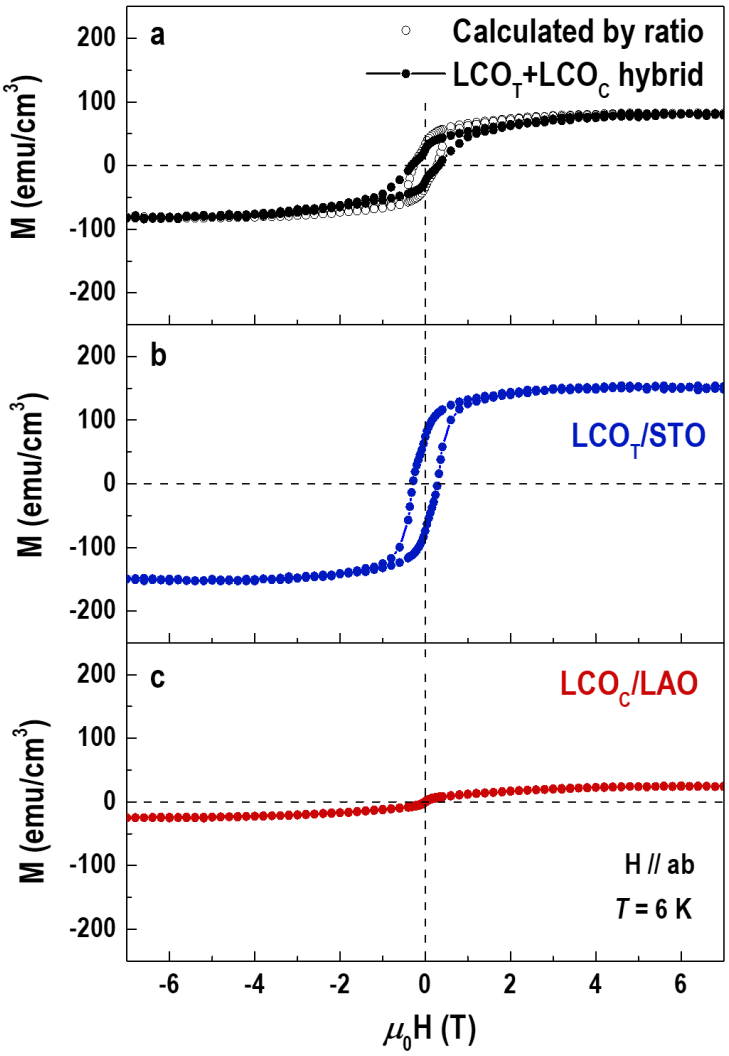

Figure S4. Magnetic hysteresis loops of (a) a LCO hybrid structure, (b) a LCO_T single film, and (c) a LCO_C single film. *M-H* curves were recorded at 6 K under in-plane magnetic fields. The LCO_T single film exhibits a typical ferromagnetic behavior, whereas the LCO_C single film does not show an apparent open hysteresis loop and saturation moment is small. These results agree with previous reports that the LCO films show ferromagnetism under tensile strain, while it exhibits suppressed long-range spin ordering under compressive strain. We further compare the averaged magnetization of a LCO hybrid structure with calculated magnetization weighted by area ratios of LCO_T (~ 40%) and LCO_C (~ 60%) layers. Both results are in reasonably good agreement in both coercive fields and saturation magnetization.

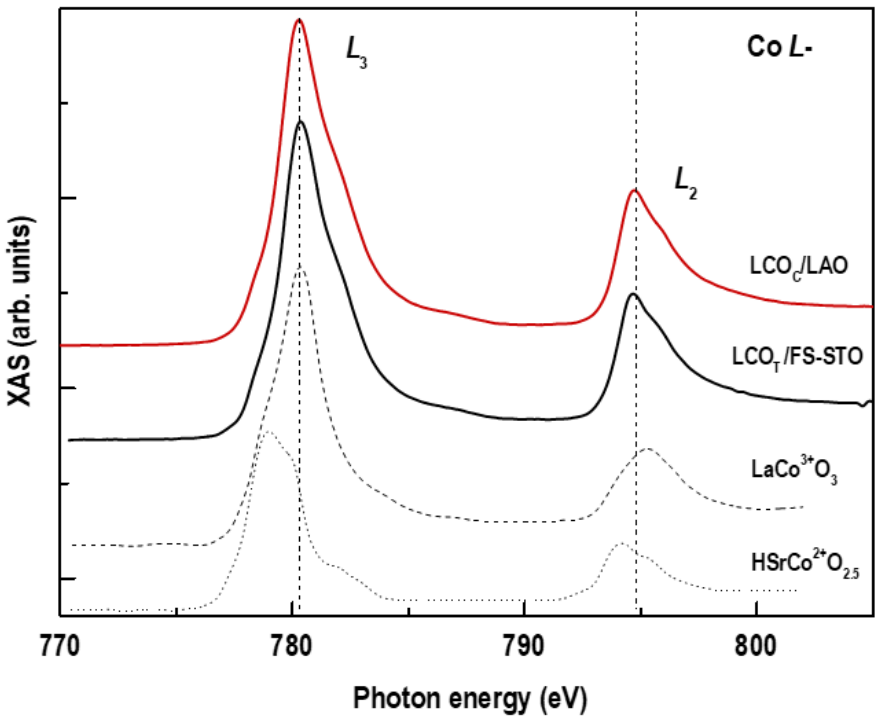

Figure S5. XAS at Co *L*-edges for LCO_C/LAO and LCO_T/FS-STO heterostructures. The spectra from different samples are shifted for clarification. The reference XAS Co *L*-edge data obtained from a LCO bulk and a $HSrCoO_{2.5}$ thin film were plotted as dashed lines. For LCO_C and LCO_T layers show strong XAS peaks at ~ 780.5 and 795 eV, in consistent with peak positions of the Co L_3- and L_2-edges for Co^{3+} ions, respectively. The valence state of Co ions is independent from strain states of LCO films, agreeing with our previous work. All spectra were collected at room temperature in TEY mode.

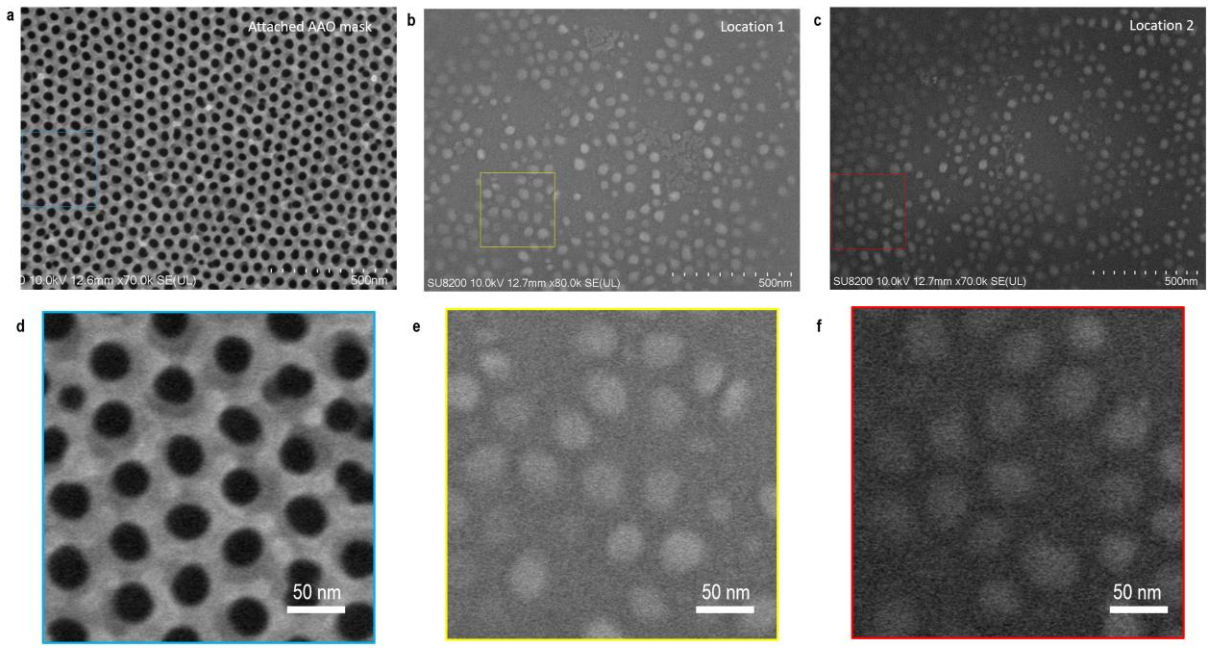

Figure S6. SEM images of nanoislands. (a) SEM image of an AAO mask attached to a LSAT substrate. (b) and (c) Two representative locations of transferred FS-STO nanoislands. (d) Zoom-in SEM image from (a). (e) and (f) Zoom-in SEM images from (b) and (e), respectively. From the scale bar within each figure, we identify that the diameters of nanoislands are ~ 30-40 nm. The averaged size of nanoislands ~ 35 nm.

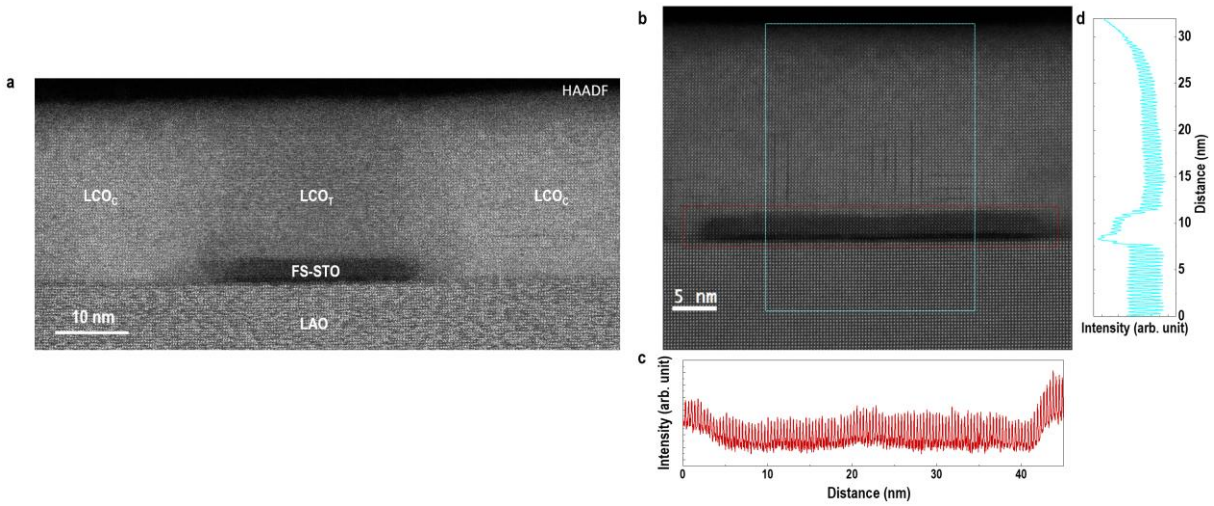

Figure S7. Structural analysis of a representative LCO nano-island. (a) Low-magnified HAADF-STEM image of an artificial LCO nano-island grown on LAO substrates. Except for FS-STO membranes, the sample show bright contrast in the STEM image due to the stronger electron scattering from La atoms. (b) Zoom-in HAADF-STEM image of an artificial LCO nano-island. Both vertical and horizontal dark stripes with a period of 3-unit-cells are observed at the LCO_T regions. (c) and (d) Intensity profiles along the in-plane and out-of-plane direction, respectively. From in-plane intensity profile, we could determine the diameter of LCO_T nano-island is (35 ± 2) nm. The thickness of FS-STO membranes is ~ 3 nm (approximately 6-7 unit cells). The gap between FS-STO membranes and LAO substrates is less than 1 nm. The structural characterizations confirm the miniature of ferromagnetic LCO_T nano domains surrounded by non-ferromagnetic LCO_C domains.

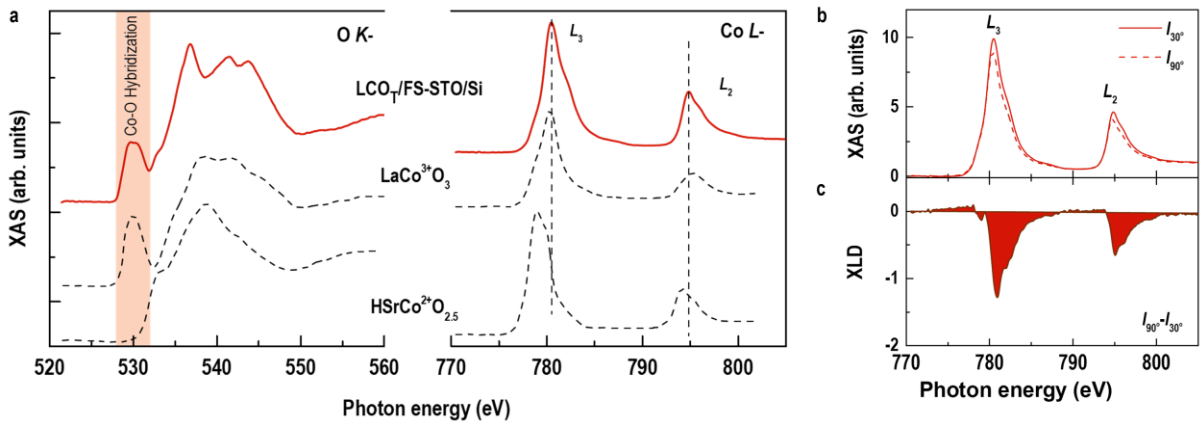

Figure S8. Electronic state of LCO$_T$/FS-STO membranes transferred on silicon. (a) XAS at O *K*- and (b) Co *L*-edges for LCO$_T$/FS-STO/Si sample. Reference data for Co^{3+} and Co^{2+} ions and their hybridization with oxygen ions were shown as dashed lines. Epitaxial growth of LCO$_T$ on FS-STO membranes does not change the valence state (+3) of Co ions. (b) XAS at Co *L*-edges when X-ray beam is parallel to the surface normal (I_{90°, solid line) or has an incident angle of 30° with respect tot the surface normal (I_{30°, dashed line). XAS represents directly the orbital occupancy in e_g bands. XAS (I_{90°) reflects the occupancy of Co $d_{3z^2-r^2}$ orbital, while XAS(I_{30°) contains both orbital information of in-plane and out-of-plane orientations. The peak energy for XAS(I_{30°) is lower than that of XAS (I_{90°), suggesting the in-plane orbitals have lower energy than the out-of-plane ones. (c) Calculated XLD ($=I_{90^\circ} - I_{30^\circ}$) for LCO$_T$/FS-STO/Si sample. The negative value of XLD demonstrates the electrons are in favor of occupying the $d_{x^2-y^2}$ orbitals rather than the $d_{3z^2-r^2}$ orbitals due to the lower energy of $d_{x^2-y^2}$ orbitals in tensile-strained LCO$_T$ layers.

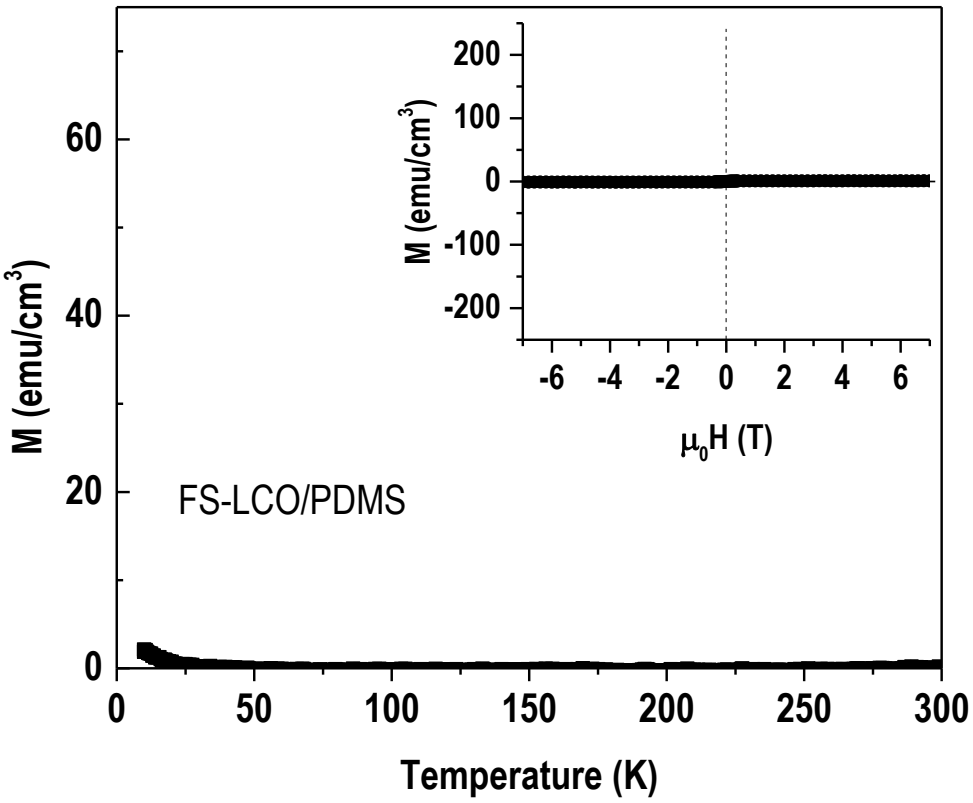

Figure S9. Magnetic properties of FS-LCO membranes on PDMS. *M-T* curve of FS-LCO membranes demonstrates no magnetic phase transition as increasing temperature. Inset shows the *M-H* curve of FS-LCO membranes. No magnetic hysteresis loop is observed. The magnetization measurements indicate FS-LCO membranes are not ferromagnetic, similar to its bulk form.

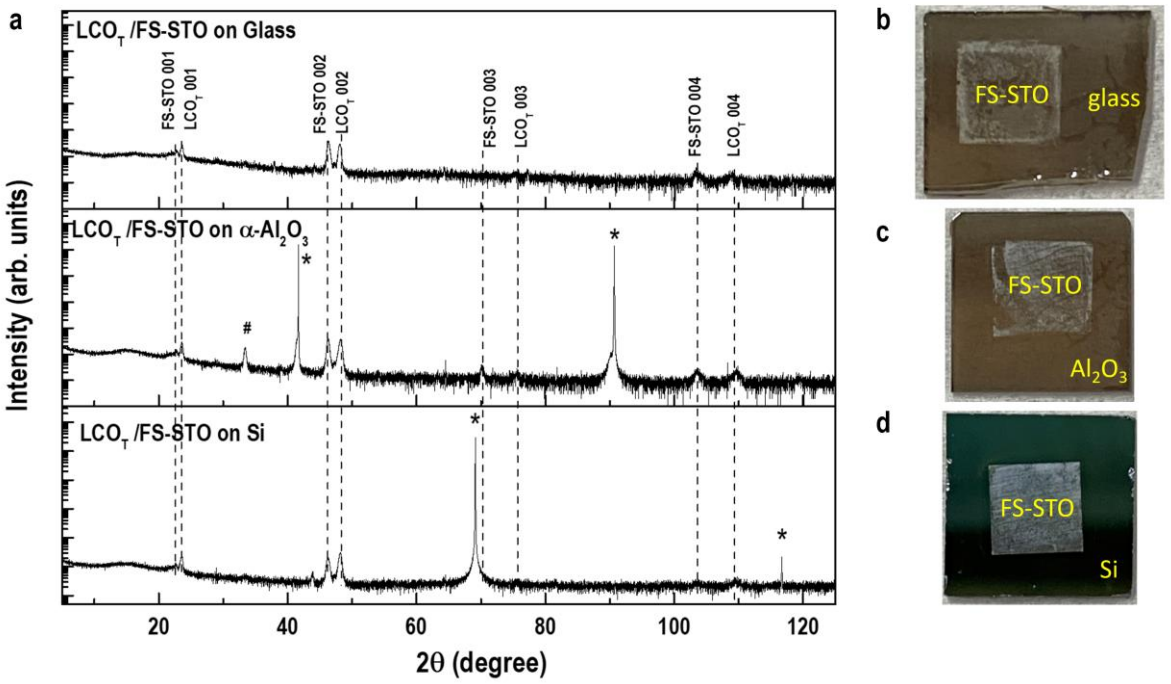

Figure S10. Epitaxy of LCO$_T$ on FS-STO membranes transferred to arbitrary substrates. (a) XRD θ-2θ scans of LCO$_T$ grown on 10nm-thick FS-STO modified glass, α-Al_2O_3, and silicon substrates. Dashed lines mark the 00*l* peak positions of LCO$_T$ layers and FS-STO membranes. "*" denotes the substrate's peaks. "#" in the middle curve identifies an undefined impurity peak. All results reinforce the epitaxial growth of LCO$_T$ layers on FS-STO membranes although the rest of LCO layers grown directly on arbitrary substrates are amorphous due to the large lattice mismatch or difference crystalline symmetries.